RSC Advances

PAPER

View Article Online
View Journal | View Issue

Cite this: *RSC Adv.*, 2022, **12**, 22377

New dimeric chromanone derivatives from the mutant strains of *Penicillium oxalicum* and their bioactivities†

Guowei Gu,‡[a] Tao Zhang,‡[a] Jianyuan Zhao,[a] Wuli Zhao,[a] Yan Tang,[ab] Lu Wang,[a] Shan Cen,[a] Liyan Yu*[a] and Dewu Zhang *[a]

Received 25th April 2022
Accepted 26th July 2022

DOI: 10.1039/d2ra02639b

rsc.li/rsc-advances

Three new chromanone dimer derivatives, paecilins F–H (**1–3**) and ten known compounds (**4–13**), were obtained from the mutant strains of *Penicillium oxalicum* 114-2. Their structures were elucidated by extensive analysis of spectroscopic data and comparison with reported data, and the configurations of **1–3** were resolved by quantum chemical calculations of NMR shifts and ECD spectra. Compounds **5** and **11** showed significant anti-influenza A virus activities with IC_{50} values of 5.6 and 6.9 μM, respectively. Compounds **8** and **9** displayed cytotoxic activities against the MIA-PaCa-2 cell line with IC_{50} values of 2.6 and 2.1 μM, respectively. Compound **10** exhibited antibacterial activities against *Bacillus cereus* with a MIC value of 4 μg mL^{-1}.

Introduction

Fungi have been demonstrated to be an important resource which could produce biologically active compounds with diverse chemical structures.[1–4] The *Penicillium* genus composed of over 200 species is one of the largest groups of fungi,[5] and a large quantity of secondary metabolites with varied architectural features and potent biological activities are isolated from *Penicillium*, including polyketides,[6–8] terpenoids,[9–11] alkaloids,[12–14] and macrolides.[15–17] The chromanone dimer is a structurally complex polyketide widely distributed in several genera of fungi, exemplified by *Aspergillus*,[18,19] *Xylaria*,[20] *Penicillium*,[21,22] *Setophoma*,[23] and *Gonytrichum*,[24,25] which display cytotoxic,[18,19] antimicrobial,[23] and innate immune-promoting[24,25] activities. In the course of investigating the biosynthesis of oxalicine B, tetrahydroxanthone dimer, secalonic acid D was isolated from the oxalicine B deletion mutant unexpectedly, which is well known for impressive anti-tumor activity. As part of our ongoing research for bioactive tetrahydroxanthone dimer derivatives from the mutant strains of *Penicillium oxalicum* 114-2, the extracts of the mutant strains of *P. oxalicum* 114-2 were investigated, which led to the isolation of thirteen polyketides, including three new dihydrochromone dimer derivatives: paecilin F (**1**), paecilin G (**2**), and paecilin H (**3**), along with ten known compounds (**4–13**) (Fig. 1). The isolated compounds were evaluated for antiviral, cytotoxic, and antibacterial activities. Herein, we describe the isolation, structural elucidation and bioactivities of these secondary metabolites from the mutants of *Penicillium oxalicum* 114-2.

Results and discussion

Compound **1** was isolated as yellow powder, and HRESI mass spectrum gave a quasi-molecular ion peak at *m*/*z* 679.1600 $[M + Na]^+$, corresponding to a molecular formula of $C_{32}H_{32}O_{15}$ with 17 degrees of unsaturation. The IR spectrum displayed absorption bands at 3422, 1783, 1676, and 1624 cm^{-1}, which indicated the existence of hydroxyl, carbonyl and aromatic moieties. The ^1H NMR spectrum (Table 1) of **1** indicated the signals of two phenolic hydroxyl protons at δ_H 11.91 (1H, s) and 11.82 (1H, s), one carboxyl protons at δ_H 12.13 (1H, br s), two sets of doublets of *ortho*-coupled aromatic protons at δ_H 7.49 (1H, d, $J = 8.4$ Hz), 6.68 (1H, d, $J = 8.4$ Hz), 7.47 (1H, d, $J = 8.4$ Hz), 6.61 (1H, d, $J = 8.4$ Hz), one hydroxyl protons at δ_H 5.73 (1H, d, $J = 6.6$ Hz), two oxymethines at δ_H 4.94 (1H, d, $J = 6.6$ Hz) and 3.89 (1H, d, $J = 5.4$ Hz), two methoxyls at δ_H 3.70 (3H, s) and 3.64 (3H, s), and two methyls at δ_H 1.18 (3H, d, $J = 7.2$ Hz), 0.93 (3H, d, $J = 6.0$ Hz). The ^{13}C NMR and DEPT spectra (Table 1) exhibited 32 carbon resonances, including sixteen non-protonated carbons (δ_C 197.2, 195.3, 175.5, 173.6, 170.4, 169.1, 159.2, 158.3, 158.2, 158.2, 140.8, 140.5, 107.2, 107.2, 87.7, and 83.8, including six carbonyl, four oxygenated aromatic, four aromatic, and two oxygenated), eight methine carbons (δ_C 140.8, 140.5, 107.2, 107.2, 81.8, 74.8, 32.6, and 30.8, including four aromatic and two oxygenated), four methylene carbons (δ_C

[a]*Institute of Medicinal Biotechnology, Chinese Academy of Medical Sciences and Peking Union Medical College, Beijing 100050, P. R. China. E-mail: yly@cpcc.ac.cn; zhangdewuever@163.com*

[b]*School of Pharmacy, Yantai University, Yantai 264005, P. R. China*

† Electronic supplementary information (ESI) available: HRESIMS, IR, UV, ECD, 1D and 2D NMR for **1–3**; cytotoxic and antibacterial activities of **1–13**. See https://doi.org/10.1039/d2ra02639b

‡ These authors have contributed equally to this work.

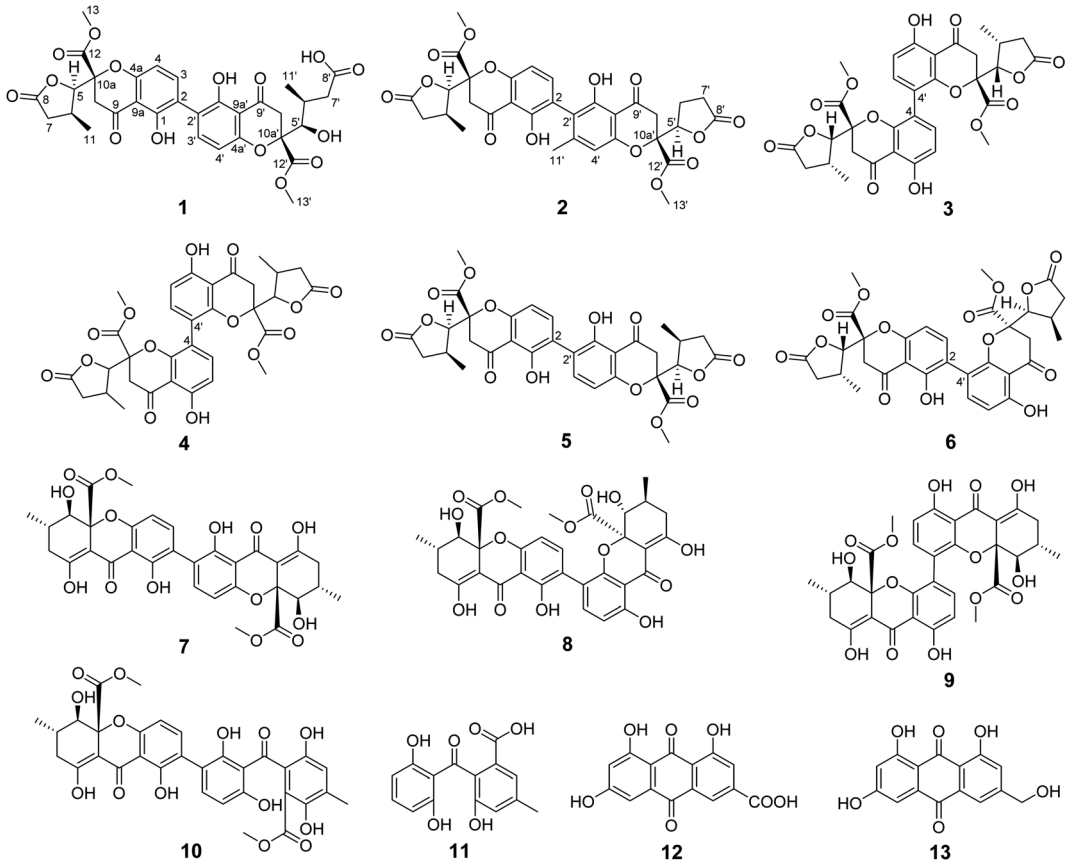

Fig. 1 Structures of compounds **1–13**.

40.3, 39.8, 39.1, and 36.7), two methoxyl carbons (δ_C 53.6 and 53.0), and two methyl carbons (δ_C 14.7 and 13.9). The ^{1}H NMR and ^{13}C NMR spectroscopic data of **1** were similar to those of paecillin D (**5**) (Tables S10 and S11†).[26] The obvious difference was that one γ-butyrolactone group in paecillin D was changed to a linear side chain in **1**, which was confirmed by the HMBC correlations (Fig. 2) from H-5′ to C-6′, C-7′, C-10′, C-10a′, C-11′, and C-12′; from H-7′ to C-5′, C-6′, C-8′, and C-11′; from 5′-OH to C-5′, C-6′, and C-10a′, along with the ^{1}H–^{1}H COSY correlations (Fig. 2) of 5′-OH/H-5′/H-6′/H-7′. Furthermore, the HMBC cross-peaks of H-3 with C-2′, H-3′ with C-2 indicated that two monomers had 2–2′ linkage. The large coupling constant of $^3J_{H\text{-}5,H\text{-}6}$ (6.6 Hz) and NOESY correlation between H-5 and H-6 established their *cis* configuration in the γ-butyrolactone group. The small coupling constant of $^3J_{H\text{-}5',H\text{-}6'}$ (1.8 Hz) and NOESY correlation between H-5′ and H-6′ indicated their gauche relationship.[19] Because the γ-butyrolactone group and flexible side chain had few effect on the ECD spectrum of **1**, a simplified

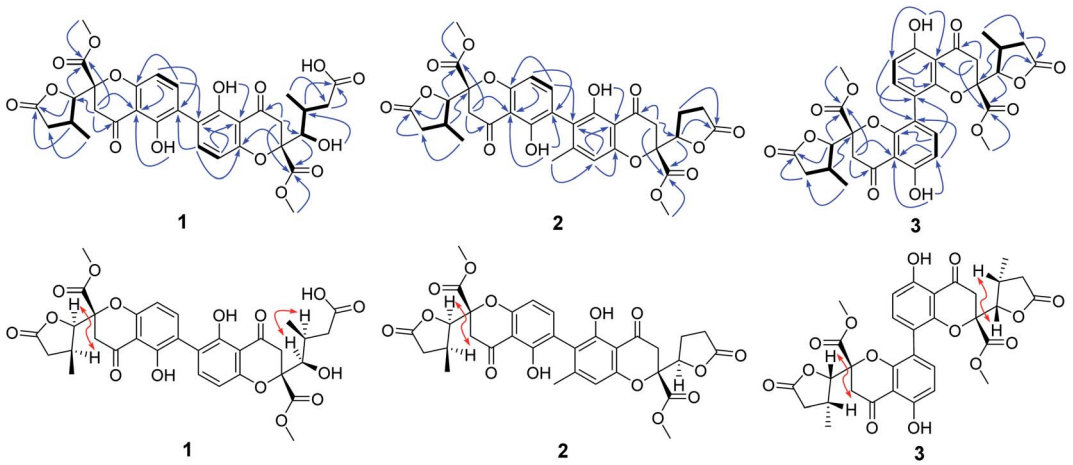

Fig. 2 Key COSY, HMBC and NOESY correlations of **1–3**.

Table 1 ^{1}H (600 MHz) and ^{13}C NMR (150 MHz) data of compounds **1–3**

	1[a]		**2**[b]		**3**[a]	
No.	δ_C	δ_H (J in Hz)	δ_C	δ_H (J in Hz)	δ_C	δ_H (J in Hz)
1	158.2, s		159.3, s		160.2, s	
2	117.0, s		116.6, s		109.5, d	6.49, d (8.4)
3	140.8, d	7.49, d (8.4)	141.7, d	7.37, d (8.4)	141.0, d	7.75, d (8.4)
4	107.2, d	6.68, d (8.4)	107.9, d	6.67, d (8.4)	114.0, s	
4a	158.3, s		159.3, s		155.4, s	
5	81.8, d	4.94, d (6.6)	82.7, d	4.80, d (6.6)	81.6, d	4.85, d (6.6)
6	32.6, d	2.98, m	33.7, d	3.00, m	32.8, d	2.88, m
7	36.7, t	2.83, dd (17.4, 8.4), 2.33, dd (17.4, 6.0)	36.8, t	2.69, dd (17.4, 8.4), 2.50, dd (17.4, 8.4)	35.8, t	2.45, dd (16.8, 8.4), 1.72, dd (16.8, 9.0)
8	175.5, s		175.0, s		174.9, s	
9	195.3, s		194.2, s		194.6, s	
9a	107.1, s		107.7, s		107.3, s	
10	39.1, t	3.61, d (17.4), 3.06, d (17.4)	40.0, t	3.27, d (17.4), 3.20, d (17.4)	39.2, t	3.56, d (18.0), 3.17, d (18.0)
10a	83.8, s		84.7, s		85.3, s	
11	14.7, q	1.18, d (7.2)	15.0, q	1.36, d (7.2)	14.3, q	1.00, d (7.2)
12	169.1, s		169.1, s		169.1, s	
13	53.6, q	3.70, s	53.7, q	3.77, s	53.6, q	3.75, s
1′	158.2, s		159.6, s		160.2, s	
2′	115.5, s		117.6, s		109.5, d	6.49, d (8.4)
3′	140.5, d	7.47, d (8.4)	151.5, s		141.0, d	7.75, d (8.4)
4′	107.2, d	6.61, d (8.4)	109.1, d	6.57, s	114.0, s	
4a′	159.2, s		158.9, s		155.4, s	
5′	74.8, d	3.89, d (5.4)	81.1, d	4.88, d (8.4, 6.0)	81.6, d	4.85, d (6.6)
6′	30.8, d	2.22, m	22.2, t	2.45, m	32.8, d	2.88, m
7	39.8, t	2.41, m, 2.19, m	27.8, t	2.72, m, 2.60, m	35.8, t	2.45, dd (16.8, 8.4), 1.72, dd (16.8, 9.0)
8′	173.6, s		175.7, s		174.9, s	
9′	197.2, s		193.2, s		194.6, s	
9a′	106.9, s		105.8, s		107.3, s	
10′	40.3, t	3.50, d (17.4), 3.01, d (17.4)	39.6, t	3.11, d (16.8), 2.97, d (16.8)	39.2, t	3.56, d (18.0), 3.17, d (18.0)
10a′	87.7, s		84.2, s		85.3, s	
11′	13.9, q	0.93, d (6.0)	21.5, q	2.12, s	14.3, q	1.00, d (7.2)
12′	170.4, s		169.1, s		169.1, s	
13′	53.0, q	3.64, s	53.9, q	3.79, s	53.6, q	3.75, s
1-OH		11.82, s		11.74, s		11.57, s
1′-OH		11.91, s		11.73, s		11.57, s
5′-OH		5.73, d, (6.6)				

[a] Recorded in DMSO-d_6. [b] Recorded in $CDCl_3$.

structure of **1A** (Fig. S1†), in which two hydroxymethyls replaced γ-butyrolactone group and butanoic acid in **1**, was used for the ECD calculations to determine the absolute configurations of C-10a and C-10a′.[27] Three stereoisomers, (10a*R*,10a′*R*)-**1Aa**, (10a*R*,10a′*S*)-**1Ab**, (10a*S*,10a′*S*)-**1Ac** existed on the basis of the relative configuration (Fig. S1†). The calculated ECD spectrum of **1Aa** was consistent with the experimental one (Fig. 3), suggesting the 10a*R*,10a′*R* configuration of **1**. Based on above-mentioned relative and absolute configurations analyses, there are four possible configurations for **1**: (5*S*,6*R*,10a*R*,5′*S*,6′*R*,10a′*R*)-**1a**, (5*S*,6*R*,10a*R*,5′*R*,6′*S*,10a′*R*)-**1b**, (5*R*,6*S*,10a*R*,5′*S*,6′*R*,10a′*R*)-**1c**, (5*R*,6*S*,10a*R*,5′*R*,6′*S*,10a′*R*)-**1d** (Fig. S3†). Subsequently, we performed computational

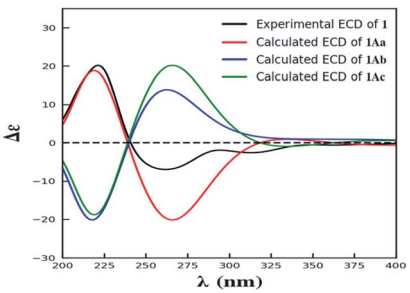

Fig. 3 The experimental ECD spectrum of **1**, and the calculated ECD spectra of **1Aa–1Ac**.

predictions of NMR chemical shifts of both the isomers **1a–1d** using the gauge-independent atomic orbital (GIAO) method at the mPW1PW91/6-311G(2d,p) level in DMSO (PCM).[28,29] Compared of the calculated ^{1}H and ^{13}C NMR data for **1a–1d** and the experimental ^{1}H and ^{13}C NMR data for **1** (Tables S1 and S2†) indicated that the possibility of structure **1b** can be excluded firstly. In addition, the correlation coefficient (R^2) obtained by linear regression analysis, corrected mean absolute deviation (CMAD), corrected largest absolute deviation (CLAD) of **1d** were superior to those of **1a** and **1c** (Table S3†), which indicated that isomer **1d** is the most reasonable configuration. Therefore, the structure of **1** was identified as paecilin F.

Compound **2** was isolated as yellow powder, and its molecular formula was established as $C_{32}H_{30}O_{14}$ based on HR-ESI peak ion *m*/*z* 677.1267 $[M + K]^+$. Its ^{1}H and ^{13}C NMR data were similar to those of paecilin D (**5**) (Tables S10 and S11†). The obvious differences include the presence of an aromatic proton at δ_H 6.57 (1H, s) and one aryl methyl moiety at δ_H 2.12 (3H, s) in **2** instead of two *ortho*-coupled aromatic protons at δ_H 7.54 (1H, d, J = 9.0 Hz), 6.63 (1H, d, J = 9.0 Hz) and a methyl moiety at δ_H 1.14 (1H, d, J = 7.2 Hz) in **5**. The HMBC correlations from H-4′ to C-2′, C-4a′, and C-9a′; from H-11′ to C-2′, C-3′, and C-4′ assigned the location of the aryl methyl group. Meanwhile, the typical methyl in one γ-butyrolactone group in **2** disappeared compared with **5**, suggesting the existence of the γ-butyrolactone group without methyl moiety in **2**, which was further determined by the ^{1}H–^{1}H COSY correlations of H-5′/H_2-6′/H_2-7′ and the HMBC correlations from H-5′ to C-6′, C-7′, C-8′, and C-12′. The large coupling constant of $^{3}J_{H\text{-}5,H\text{-}6}$ (6.6 Hz) and NOESY correlation between H-5 and H-6 indicated their *cis* configuration in the γ-butyrolactone group. The similar positive Cotton effect around 214 nm and negative Cotton effect around 245 nm (Fig. S31†) compared to those of **1** suggested the 10a*R*,10a′*R* absolute configuration of **2**. To assign the configurations of C-5, C-6, and C-5′, quantum chemical calculations of the NMR data of four diastereoisomers: (5*S*,6*R*,10a*R*,5′*S*,10a′*R*)-**2a**, (5*S*,6*R*,10a*R*,5′*R*,10a′*R*)-**2b**, (5*R*,6*S*,10a*R*,5′*S*,10a′*R*)-**2c**, (5*R*,6*S*,10a*R*,5′*R*,10a′*R*)-**2d** (Fig. S4†), were performed using GIAO method at the mPW1PW91/6-311G(2d,p) level in chloroform (PCM).[28,29] The calculated chemical shifts of **2a–2d** (Tables S4 and S5†), especially the calculated NMR data of **2d**, were in good agreement with the experimental values. Moreover, the R^2, CMAD, and CLAD values of **2d** were superior to those of **2a–2c** (Tables S6†). The deduction was further supported by DP4+ probability analysis (Fig. S8†), which showed that isomer **2d** was the most reasonable configuration with a probability of 99.84% for the combination of ^{1}H and ^{13}C NMR data. These results indicated that the configuration of **2d** was the most plausible. Accordingly, the structure of **2** was elucidated to be paecilin G.

Compound **3** was obtained as yellow powder. The molecular formula was determined to be $C_{32}H_{30}O_{14}$ by HR-ESI mass spectrum, which showed a quasi-molecular ion peak at *m*/*z* 639.1677 $[M + H]^+$. Its ^{1}H and ^{13}C NMR spectroscopic data were great similar to those of paecilin A (**4**).[30] Interpretation of its 1D and 2D NMR data of **3** established the same planar structure as **4**. A literature search revealed that a total of five stereoisomers for **3** have been reported: paecilin A (**4**), paecilin C (**3A**),[21] dimethyl (2*S*,2′*S*)-5,5′-dihydroxy-2,2′-bis[(2*S*,3*S*)-3-methyl-5-oxotetrahydrofuran-2-yl]4,4′-dioxo-[8,8′-bichroman]-2,2′-dicarboxylate (**3B**),[31] dimethyl (2*S*,2′*S*)-5,5′-dihydroxy-2,2′-bis([2*R*,3*R*]-3-methyl-5-oxotetrahydrofuran-2-yl)-4,4′-dioxo-[8,8′-bichromane]-2,2′-dicarboxylate (**3C**),[32] dimethyl (2*S*,2′*S*)-5,5′-dihydroxy-2-([2*S*,3*S*]-3-methyl-5-oxotetrahydrofuran-2-yl)-2′-([2*R*,3*R*]-3-methyl-5-oxotetrahydrofuran-2-yl)-4,4′-dioxo-[8,8′-bichromane]-2,2′-dicarboxylate (**3D**) (Fig. S9†).[32] Detailed analysis of NMR data of these stereoisomers indicated that **3** was new chromanone dimer (Tables 1, S12, and S13†). The large coupling constant of $^{3}J_{H\text{-}5,H\text{-}6}$ (6.6 Hz) and $^{3}J_{H\text{-}5',H\text{-}6'}$ (6.6 Hz), as well as NOESY correlation between H-5 and H-6 indicated their *cis* configuration in the γ-butyrolactone group. The absolute configuration of C-10a and C-10a′ in **3** was determined as described for **1** by comparison of its experimental and calculated ECD spectra. Similarly, a simplified structure **3A** was subjected to ECD calculations.[27] Only two possible stereoisomers for **3**: (10a*S*,10a′*S*)-**3Aa** and (10a*R*,10a′*R*)-**3Ab**, remained on the basis of its NMR data (Fig. S5†). The calculated ECD spectrum of **3Ab** was consistent with the experimental one (Fig. 4), establishing the 10a*R*,10a′*R* absolute configuration of **3**. After the relative configuration analysis, there are two diastereoisomers: (5*R*,6*S*,10a*R*,5′*R*,6′*S*,10a′*R*)-**3a**, (5*S*,6*R*,10a*R*,5′*S*,6′*R*,10a′*R*)-**3b** (Fig. S7†). Chemical shifts of isomers **3a** and **3b** were predicted using the GIAO method at the mPW1PW91/6-311G(2d,p) level in DMSO.[28,29] The calculated ^{1}H and ^{13}C NMR data of **3b** matched well with the experimental values (Tables S7 and S8†), and the R^2, CMAD, and CLAD values of calculated ^{1}H NMR data for **3b** were also superior to those of **3a** (Tables S9†), indicating the configuration of **3b** was more reasonable than **3a**. Thus, the structure of **3** was determined to be paecilin H.

Additionally, we analyzed the coupling constant of $^{3}J_{H\text{-}5,H\text{-}6}$ for **1–6** and those of its stereoisomers reported in the literature (Table 1, S11 and S12†),[21,26,30–33] indicating that the large coupling constant of $^{3}J_{H\text{-}5,H\text{-}6}$ (J > 6 Hz) assigned the *cis* configuration of γ-butyrolactone group, and small coupling constant of $^{3}J_{H\text{-}5,H\text{-}6}$ (J < 5 Hz) established the *trans* configuration of γ-butyrolactone group, which can provide guidance for determining the relative configuration of C-5 and C-6 for chromanone dimer and monomer derivatives.

The known compounds were identified as paecilin A (**4**),[30] paecilin D (**5**),[26] paecilin E (**6**),[33] secalonic acid D (**7**),[34] 2,4′-secalonic acid D (**8**),[35] 4,4′-secalonic acid D (**9**),[36] secalonic acid

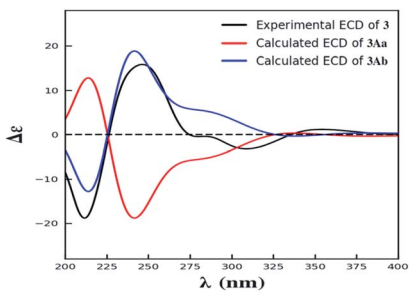

Fig. 4 The experimental ECD spectrum of **3**, and the calculated ECD spectra of **3Aa** and **3Ab**.

Table 2 The anti-IAV activities of **1–13**

Compounds	Inhibition rate (%) in 10 μM	IC_{50} (μM)	CC_{50} (μM)	SI
1	23.5 ± 1.0	—	—	
2	27.1 ± 3.1	—	—	
3	18.7 ± 6.1	—	—	
4	27.1 ± 4.6	—	—	
5	90.8 ± 2.1	5.6 ± 0.7	46.2 ± 2.0	8.3
6	16.4 ± 1.5	—	—	
7	74.7 ± 7.1	—	12.2 ± 1.2	
8	65.5 ± 3.1	—	10.5 ± 3.4	
9	49.6 ± 5.4	—	13.2 ± 2.5	
10	40.2 ± 7.4	—	—	
11	97.2 ± 1.8	6.9 ± 1.1	>100	>14.5
12	15.0 ± 4.8	—	—	
13	49.9 ± 1.0	—	—	
Ribavirin	90.3 ± 5.2 (50 μM)	28.2 ± 4.4	>100	>3.5

H (**10**),[22] monodictyphenone (**11**),[37] emodic acid (**12**),[38] and citreorosein (**13**)[39] by comparison of their NMR and MS data with those reported in the literatures.

Compounds **1–13** were evaluated for anti-influenza A virus (IAV), cytotoxic, and antibacterial activities. Compounds **5** and **11** exhibited significant anti-IAV (A/WSN/33, H1N1) activities with the IC_{50} values of 5.6 and 6.9 μM, respectively (Table 2). Compounds **8** and **9** displayed cytotoxic activities against MIA-PaCa-2 cell line with the IC_{50} values of 2.6 and 2.1 μM, respectively (Table S14†). Compounds **1–13** were tested for antibacterial activities against *Escherichia coli* ATCC 25922, *Enterococcus faecalis* ATCC 29212, *Pseudomonas syringae* CPCC 101099, *Bacillus cereus* CPCC 101254, *Acinetobacter baumannii* 12-8, *Pseudomonas aeruginosa* 13-17, *Klebsiella pneumoniae* ATCC BAA-2146, *Enterococcs faecium* ATCC 700221 and *Staphylococcus aureus* ATCC 33591. Compounds **8** and **10** exhibited moderate antibacterial activities against *Bacillus cereus* CPCC 101254 with the MIC values of 32 μg mL^{-1} and 4 μg mL^{-1}, respectively, and others showed no antibacterial activities (Table S15†).

Conclusions

In conclusion, thirteen secondary metabolites including three new chromanone dimers, paecilins F–H (**1–3**) were isolated from the mutants of *Penicillium oxalicum* 114-2. Their structures were elucidated by detailed interpretation of the spectroscopic data, and the stereochemistry of **1–3** were established by computational predictions of NMR chemical shifts and calculated ECD spectra. Compounds **5** and **11** displayed significant anti-IAV activities with IC_{50} values of 5.6 and 6.9 μM, respectively, which were stronger than the positive control, ribavirin (IC_{50} = 28.2 μM), indicating that **5** and **11** might be promising natural agents for antiviral drug discovery.

Experimental

General experimental procedures

Optical rotations were recorded on an Autopol IV automatic polarimeter with a 10 cm glass microcell at 25 °C (Rudolph Research Analytical, NJ, USA). The CD spectra were measured on a JASCO J-815 spectropolarimeter using CH_3OH as the solvent at room temperature (Jasco Corporation, Tokyo, Japan). UV spectra were obtained in CH_3OH on a Persee TU-1901 UV-vis spectrometer (Beijing Purkinje General Instrument Co., Ltd, Beijing, China). IR spectra were acquired on a PerkinElmer FT-IR/NIR spectrometer (PerkinElmer, Waltham, MA, USA). 1D and 2D NMR spectra were performed at 600 MHz for ^1H NMR and 150 MHz for ^{13}C NMR on Bruker ARX-600 spectrometer using solvent signals as the internal standard (Bruker, Switzerland). Chemical shifts (δ) are given in ppm, and coupling constants (J) are given in hertz (Hz). ESIMS data were recorded on a Thermo LTQ mass spectrometer (Thermo Fisher Scientific, Waltham, MA, USA). HRESIMS data were measured using a Thermo LTQ Orbitrap XL mass spectrometer (Thermo Fisher Scientific, Waltham, MA, USA). Column chromatography (CC) were carried out with silica gel (200–300 mesh, Qingdao Marine Chemical Inc. Qingdao, PR China). Analytical TLC was carried out on pre-coated silica gel GF_{254} plates (Qingdao Marine Chemical Industry, Qingdao, China), and spots were visualized under UV light or by spraying with 10% H_2SO_4 in 90% EtOH followed by heating at 120 °C.

Fungal material

The wild type strain *P. oxalicum* 114-2 was kindly provided by Prof Qu Yinbo from National Glycoengineering Research Center, Shandong University.[40] The oxalicine B deletion mutants derived from parental strain 114-2 including Δ*oxaB*, Δ*oxaL*, and Δ*oxaK* were obtained during our research on biosynthesis of oxalicine B. All the strains used in this study are deposited in the China Pharmaceutical Culture Collection (CPCC), Institute of Medicinal Biotechnology, Chinese Academy of Medical Sciences and Peking Union Medical College.

Fermentation, extraction and isolation

The fungal strain was spread onto slants of PDA medium (potato starch 0.4%, dextrose 2.0%, agar 1.5%; the media were autoclaved at 121 °C for 15 min), and incubated at 28 °C for 5–7 days to generate spores. The spores were inoculated in PDA plate medium at 28 °C for 5 days to prepare spore suspension (seed culture). Fermentation was carried out on plate, each plate

contained about 50 ml medium (2% malt extract broth, 2% agar and 0.2% soybean meal, autoclaving at 121 °C for 30 min). After cooling to solid medium, each plate was added into 200 μL of the spore suspension, coating evenly, and incubated at 28 °C for 7 days.

The fermented material was extracted repeatedly with EtOAc (3 × 3 L), and the organic solvent was evaporated to dryness under vacuum to yield the crude extract, which was initially subjected to silica gel (Qingdao Marine Chemical Inc. Qingdao, China) column chromatography (CC) eluting with dichloromethane–acetone gradient (100 : 0–0 : 100, v/v) to produce six fractions (Fr.1–Fr.6) based on the HPLC analysis. Fr.2–Fr.4 and Fr.6 were subjected to reversed-phase silica gel column chromatography eluting with CH_3CN–H_2O gradient (10 : 90–100 : 0, v/v), respectively. Fr.2.2 (30 mg) was subjected to Sephadex LH-20 CC to give compound **11** (3 mg). Fr.2.4 (16 mg) was purified by reversed-phase semi-preparative HPLC eluting with CH_3CN–H_2O (0.1% TFA) (45 : 55) at 4 ml min^{-1} to yield **13** (2.0 mg, t_R = 8.5 min) and **12** (3.0 mg, t_R = 18 min). Fr.3.2 (7 mg) was purified by reversed-phase semi-preparative HPLC eluting with CH_3CN–H_2O (0.1% TFA) (40 : 60) at 4 ml min^{-1} to yield **1** (1.2 mg, t_R = 22.6 min). Fr.3.4 (40 mg) was subjected to Sephadex LH-20 CC to produce four fractions (Fr.3.4.1–Fr.3.4.4). Fr.3.4.2 (9 mg) was purified by reversed-phase semi-preparative HPLC eluting with CH_3CN–H_2O (0.1% TFA) (40 : 60, v/v) at 4 ml min^{-1} to obtain **2** (1.4 mg, t_R = 33.4 min). Fr.3.4.3 (22 mg) was purified by reversed-phase semi-preparative HPLC eluting with CH_3CN–H_2O (0.1% TFA) gradient (40 : 60–100 : 0, v/v) at 4 ml min^{-1} to obtain **3** (4 mg, t_R = 20.9 min). Fr.4.2 (46 mg) was subjected to Sephadex LH-20 CC to produce four fractions (Fr.4.2.1–Fr.4.2.4). Fr.4.2.1 (15 mg) was purified by reversed-phase semi-preparative HPLC eluting with CH_3CN–H_2O (50 : 50, v/v) at 4 ml min^{-1} to obtain **5** (8 mg, t_R = 17.0 min). Fr.4.2.3 (10 mg) was purified by reversed-phase semi-preparative HPLC eluting with CH_3CN–H_2O (0.1% TFA) gradient (45 : 55–100 : 0, v/v) at 4 ml min^{-1} to obtain **10** (3.5 mg, t_R = 18.3 min). Fr.4.2.4 (11 mg) was purified by reversed-phase semi-preparative HPLC eluting with CH_3CN–H_2O (0.1% TFA) gradient (45 : 55–100 : 0, v/v) at 4 ml min^{-1} to obtain **4** (1.5 mg, t_R = 17.0 min). Fr.4.3 (14 mg) was purified by reversed-phase semi-preparative HPLC eluting with CH_3CN–H_2O (45 : 55, v/v) at 4 ml min^{-1} to obtain **6** (3.3 mg, t_R = 32.4 min). Fr.5 subjected to recrystallization to obtain **7** (1.1 g). Fr.6.2 (380 mg) was purified by reversed-phase semi-preparative HPLC eluting with CH_3CN–H_2O (0.1% TFA) gradient (50 : 50–100 : 0 for, v/v) at 4 ml min^{-1} to obtain **9** (15 mg, t_R = 17.9 min) and **8** (26 mg, t_R = 18.0 min).

Paecilin F (1). Yellow power. $C_{32}H_{32}O_{15}$; $[\alpha]_D^{25}$ −195.45 (*c* 0.044, $CHCl_3$); UV (MeOH) λ_{max} (log ε): 206 (2.03), 257 (1.46) and 364 (0.49) nm; IR ν_{max}: 3422, 2925, 1783, 1734, 1676, 1624, 1433, 1357, 1202, 1135, 800 and 722 cm^{-1}; CD (MeOH) λ_{max} ($\Delta\varepsilon$): 221.5 (+20.17), 261.5 (−6.98), 313.5 (−2.59) nm; ESIMS *m*/*z*: 657.46 $[M + H]^+$; HR-ESIMS *m*/*z*: 679.16003 $[M + Na]^+$ (calcd for $C_{32}H_{32}NaO_{15}$, 679.16334); ^1H and ^{13}C NMR data, see Table 1.

Paecilin G (2). Yellow power. $C_{32}H_{30}O_{14}$; $[\alpha]_D^{25}$ −21.67 (*c* 0.06, $CHCl_3$); UV (MeOH) λ_{max} (log ε): 206 (1.65), 276 (0.83) and 360 (0.36) nm; IR ν_{max}: 3421, 2923, 1787, 1677, 1646, 1456, 1435, 1203, 1136, 1027, 802 and 724 cm^{-1}; CD (MeOH) λ_{max} ($\Delta\varepsilon$): 214.0 (+12.62), 245.0 (−5.00), 281.5 (−2.48), 382.0 (+0.52) nm; ESIMS *m*/*z*: 639.54 $[M + H]^+$; HR-ESIMS *m*/*z*: 677.12360 $[M + K]^+$ (calcd for $C_{32}H_{30}KO_{14}$, 677.12671). ^1H and ^{13}C NMR data, see Table 1.

Paecilin H (3). Yellow power. $C_{32}H_{30}O_{14}$; $[\alpha]_D^{25}$ +51.92 (*c* 0.052, $CHCl_3$); UV (MeOH) λ_{max} (log ε): 208 (2.26), 254 (1.84) and 360 (0.52) nm; IR ν_{max}: 3420, 2980, 1789, 1741, 1650, 1587, 1463, 1345, 1278, 1228, 1202, 1158, 1025, 998 and 736 cm^{-1}; CD (MeOH) λ_{max} ($\Delta\varepsilon$) 211.5 (−18.83), 246.5 (+15.85), 309.0 (−3.21), 354.5 (+1.17) nm; ESIMS *m*/*z*: 639.43 $[M + H]^+$; HR-ESIMS *m*/*z*: 639.16766 $[M + H]^+$ (calcd for $C_{32}H_{31}O_{14}$, 639.17083). ^1H and ^{13}CNMR data, see Table 1.

ECD calculations

The simplified structures **1A** and **3A** (Fig. S1 and S5†) were used as the model compounds of **1** and **3**, respectively. Conformational analyses of **1A** and **3A** were performed by using the MMFF94 molecular mechanics force field. According to the relative energy within 6 kcal mol^{-1}, the molecules of **1Aa**, **1Ab**, and **3Aa** showed 9 and 7 conformers with distributions higher than 1%, respectively (Fig. S2 and S6†). The resultant conformers were further optimized and checked as the true minima of potential energy surface by the density functional theory method at the B3LYP/6-31G(d) level, and 30 lowest electronic transitions were calculated. ECD spectra of different conformers were simulated using a Gaussian function with a half-bandwidth of 0.4 eV. The overall theoretical ECD spectra were given on the basis of the Boltzmann weighting of each conformers. In the 200–400 nm region, the theoretically calculated ECD and UV spectra of **1A** and **3A** compared with the experimental ECD data of **1** and **3**, which led the assignment of the absolute configurations of C-10a and C-10a′ for **1** and **3**.[27]

Quantum chemical calculations

All theoretical calculations were carried out using the Gaussian 09 program package. Conformation search by MMFF94 molecular force fields with 6 kcal mol^{-1} energy window limit was performed for all possible isomers, providing corresponding stable conformers with distributions higher than 1%. The conformers were optimized using the semiempirical PM6 method available in Gaussian 09 software package. The resulting geometries were further optimized at the HF/6-31G(d) and B3LYP/6-31G9d levels of theory in the gas phase. The predominant conformers were subjected to theoretical NMR calculations at the mPW1PW91/6-311G(2d,p) level of theory. The Boltzmann distributions were performed using the Gibbs free energies as weighting factors. The linear regression approach was used to convert NMR shielding tensors into NMR chemical shifts, and the NMR chemical shifts were considered as the average values of the same atoms in the different conformers. The theoretical NMR data were statistically analyzed with experimental chemical shifts, using DP4+ probability.[28,29]

Anti-IAV activity assays

All the metabolites were evaluated for their anti-IAV activities as previously described methods.[41]

Cytotoxic activity assays

All the metabolites were tested for their cytotoxic activities as previously reported methods.[42]

Antibacterial activity assays

All the metabolites were tested for their antibacterial activities as previously described methods.[41]

Conflicts of interest

There are no conflicts to declare.

Acknowledgements

This research was funded by the National Natural Science Foundation of China (82073744, 31872617), CAMS Innovation Fund for Medical Sciences (2021-I2M-1-055, 2019-I2M-1-005), the National Mega-project for Innovative Drugs (2019ZX09721001-004-006), and the National Microbial Resource Center (NMRC-2021-3). We thank the CAMS Collection Center of Pathogenic Microorganisms (CAMS-CCPM-A) for providing valuable reagents. We are grateful to Prof. Qu Yinbo (National Glycoengineering Research Center, Shandong University, Jinan, China) for sharing the strain *P. oxalicium* 114-2.

Notes and references

1 S. Chen, R. Cai, Z. Liu, H. Cui and Z. She, *Nat. Prod. Rep.*, 2022, **39**, 560–595.
2 T. El-Elimat, H. A. Raja, M. Figueroa, A. H. Al Sharie, R. L. Bunch and N. H. Oberlies, *J. Nat. Prod.*, 2021, **84**, 898–916.
3 A. Schueffler and T. Anke, *Nat. Prod. Rep.*, 2014, **31**, 1425–1448.
4 X. Yang, J. Liu, J. Mei, R. Jiang, S. Tu, H. Deng, J. Liu, S. Yang and J. Li, *Mini-Rev. Med. Chem.*, 2021, **21**, 2000–2019.
5 R. M. K. Toghueo and F. F. Boyom, *3 Biotech.*, 2020, **10**, 107.
6 J. Xue, H. Li, P. Wu, L. Xu, Y. Yuan and X. Wei, *J. Nat. Prod.*, 2020, **83**, 1480–1487.
7 Z. F. Wang, Z. C. Sun, L. Xiao, Y. M. Zhou and F. Y. Du, *J. Agric. Food Chem.*, 2019, **67**, 14102–14109.
8 T. Asai, D. Luo, K. Yamashita and Y. Oshima, *Org. Lett.*, 2013, **15**, 1020–1023.
9 N. P. Ariantari, E. Ancheeva, C. Wang, A. Mándi, T. O. Knedel, T. Kurtán, C. Chaidir, W. E. G. Müller, M. U. Kassack, C. Janiak, G. Daletos and P. Proksch, *J. Nat. Prod.*, 2019, **82**, 1412–1423.
10 J. W. Tang, L. M. Kong, W. Y. Zu, K. Hu, X. N. Li, B. C. Yan, W. G. Wang, H. D. Sun, Y. Li and P. T. Puno, *Org. Lett.*, 2019, **21**, 771–775.
11 H. L. Li, R. Xu, X. M. Li, S. Q. Yang, L. H. Meng and B. G. Wang, *Org. Lett.*, 2018, **20**, 1465–1468.
12 D. Zhang, L. Zhao, L. Wang, X. Fang, J. Zhao, X. Wang, L. Li, H. Liu, Y. Wei, X. You, S. Cen and L. Yu, *J. Nat. Prod.*, 2017, **80**, 371–376.
13 L. H. Meng, C. Y. Wang, A. Mándi, X. M. Li, X. Y. Hu, M. U. Kassack, T. Kurtán and B. G. Wang, *Org. Lett.*, 2016, **18**, 5304–5307.
14 T. Song, M. Chen, Z. W. Ge, W. Chai, X. C. Li, Z. Zhang and X. Y. Lian, *J. Org. Chem.*, 2018, **83**, 13395–13401.
15 Y. Zhang, J. Bai, L. Zhang, C. Zhang, B. Liu and Y. Hu, *Angew. Chem., Int. Ed. Engl.*, 2021, **60**, 6639–6645.
16 L. H. Meng, X. M. Li, C. T. Lv, C. S. Li, G. M. Xu, C. G. Huang and B. G. Wang, *J. Nat. Prod.*, 2013, **76**, 2145–2149.
17 M. Okabe, T. Sugita, K. Kinoshita and K. Koyama, *J. Nat. Prod.*, 2016, **79**, 1208–1212.
18 G. Wu, X. Qi, X. Mo, G. Yu, Q. Wang, T. Zhu, Q. Gu, M. Liu, J. Li and D. Li, *Eur. J. Med. Chem.*, 2018, **148**, 268–278.
19 G. Wu, G. Yu, T. Kurtán, A. Mándi, J. Peng, X. Mo, M. Liu, H. Li, X. Sun, J. Li, T. Zhu, Q. Gu and D. Li, *J. Nat. Prod.*, 2015, **78**, 2691–2698.
20 A. Maha, V. Rukachaisirikul, S. Phongpaichit, W. Poonsuwan and J. Sakayaroj, *Tetrahedron*, 2016, **72**, 2874–2879.
21 J. Bao, Y. L. Sun, X. Y. Zhang, Z. Han, H. C. Gao, F. He, P. Y. Qian and S. H. Qi, *J. Antibiot.*, 2013, **66**, 219–223.
22 L. Chen, Y. X. Bi, Y. P. Li, X. X. Li, Q. Y. Liu, M. G. Ying, Q. H. Zheng, L. Du and Q. Q. Zhang, *Heterocycles*, 2017, **94**, 1766–1774.
23 T. El-Elimat, M. Figueroa, H. A. Raja, T. N. Graf, S. M. Swanson, J. O. Falkinham 3rd, M. C. Wani, C. J. Pearce and N. H. Oberlies, *Eur. J. Org. Chem.*, 2015, **2015**, 109–121.
24 H. Kikuchi, M. Isobe, M. Sekiya, Y. Abe, T. Hoshikawa, K. Ueda, S. Kurata, Y. Katou and Y. Oshima, *Org. Lett.*, 2011, **13**, 4624–4627.
25 H. Kikuchi, M. Isobe, S. Kurata, Y. Katou and Y. Oshima, *Tetrahedron*, 2012, **68**, 6218–6223.
26 P. H. F. da Silva, M. P. de Souza, E. A. Bianco, S. R. S. da Silva, L. N. Soares, E. V. Costa, F. M. A. da Silva, A. Barison, M. R. Forim, Q. B. Cass, A. D. L. de Souza, H. H. F. Koolen and A. Q. L. de Souza, *J. Braz. Chem. Soc.*, 2017, **29**, 622–630.
27 D. Zhang, X. Tao, R. Chen, J. Liu, L. Li, X. Fang, L. Yu and J. Dai, *Org. Lett.*, 2015, **17**, 4304–4307.
28 S. G. Smith and J. M. Goodman, *J. Org. Chem.*, 2009, **74**, 4597–4607.
29 M. W. Lodewyk, M. R. Siebert and D. J. Tantillo, *Chem. Rev.*, 2012, **112**, 1839–1862.
30 Z. Guo, Z. She, C. Shao, L. Wen, F. Liu, Z. Zheng and Y. Lin, *Magn. Reson. Chem.*, 2007, **45**, 777–780.
31 L. F. Tietze, L. Ma, S. Jackenkroll, J. R. Reiner, J. Hierold, B. Gnanaprakasam and S. Heidemann, *Heterocycles*, 2014, **88**, 1101–1119.
32 G. Valdomir, S. Senthilkumar, D. Ganapathy, Y. Zhang and L. F. Tietze, *Chem.–Asian J.*, 2018, **13**, 1888–1891.
33 D. Kumla, T. S. Aung, S. Buttachon, T. Dethoup, L. Gales, J. A. Pereira, Â. Inácio, P. M. Costa, M. Lee, N. Sekeroglu, A. M. S. Silva, M. M. M. Pinto and A. Kijjoa, *Mar. Drugs*, 2017, **15**, 375.
34 H. Ren, L. Tian, Q. Gu and W. Zhu, *Arch. Pharmacal Res.*, 2006, **29**, 59–63.

35 T. Qin, T. Iwata, T. T. Ransom, J. A. Beutler and J. A. Porco Jr, *J. Am. Chem. Soc.*, 2015, **137**, 15225–15233.
36 L. Chen, Y. P. Li, X. X. Li, Z. H. Lu, Q. H. Zheng and Q. Y. Liu, *J. Antibiot.*, 2019, **72**, 34–44.
37 B. Liu, H. F. Wang, L. H. Zhang, F. Liu, F. J. He, J. Bai, H. M. Hua, G. Chen and Y. H. Pei, *Chem. Nat. Compd.*, 2016, **52**, 821–823.
38 K. A. Alvi, B. Nair, C. Gallo and D. Baker, *J. Antibiot.*, 1997, **50**, 264–266.
39 J. L. Liang, H. C. Cha, S. H. Lee, J. K. Son, H. W. Chang, J. E. Eom, Y. Kwon and Y. Jahng, *Arch. Pharmacal Res.*, 2012, **35**, 447–454.
40 G. Yao, R. Wu, Q. Kan, L. Gao, M. Liu, P. Yang, J. Du, Z. Li and Y. Qu, *Biotechnol. Biofuels*, 2016, **9**, 78.
41 D. Zhang, G. Gu, B. Zhang, Y. Wang, J. Bai, Y. Fang, T. Zhang, S. Dai, S. Cen and L. Yu, *RSC Adv.*, 2021, **11**, 22489–22494.
42 D. Zhang, X. Tao, G. Gu, Y. Wang, W. Zhao, W. Zhao, Y. Ren, S. Dai and L. Yu, *Front. Microbiol.*, 2021, **12**, 662321.